

COMPASS results on inclusive and semi-inclusive polarised DIS

Helena Santos¹, on behalf of the COMPASS Collaboration

(1) *LIP - Laboratório de Instrumentação e Física Experimental de Partículas*
Av. Elias Garcia, 14, 1000-149, Lisboa, Portugal

Abstract

The COMPASS experiment at the CERN SPS has an extensive experimental program focused on the nucleon structure and on hadron spectroscopy. A main topic of investigation is the spin structure of the nucleon via deep-inelastic scattering of 160 GeV polarised muons on polarised nucleons. Results obtained in the kinematic ranges $Q^2 < 1$ (GeV/c)² and $0.0005 < x < 0.02$, as well as $1 < Q^2 < 100$ GeV² and $0.004 < x < 0.7$ are shown. The results of a global QCD fit at NLO to the world g_1 data are discussed. Then, the evaluation of the polarised valence quark distributions $\Delta u_v(x) + \Delta d_v(x)$ is presented. The analysis is based on the difference asymmetry, $A^{(h^+ - h^-)}$, for hadrons of opposite charges. This approach gives direct access to the valence quark helicity distributions, as the fragmentation functions do cancel out in LO QCD. The results derived provide information about the contribution of the sea quarks to the nucleon spin. Comparison with SMC and HERMES results is also shown.

1 Introduction

The investigation of the spin structure of the nucleon begun more than 30 years ago with polarised deep inelastic scattering measurements at SLAC [1]. At that time the quark-parton model and the analyses on weak baryon decays have predicted that 60% of the nucleon spin was entirely given by the u and d quarks [2]. The first experimental results supported this prediction but were obtained at a poor x range ($x > 0.1$). The EMC Collaboration extended the measurements to $x > 0.01$ and came out with the unexpected value of $0.12 \pm 0.09 \pm 0.14$ [3]. Such a result motivated a series of experiments covering different x ranges at CERN [4], SLAC [5, 6, 7, 8], DESY [9] and JLAB [10]. All these experiments confirmed the small contribution of the quarks (about 20–30%) to the nucleon spin, and thus more contributions are necessary. For a nucleon with $+1/2$ helicity one has the sum rule:

$$S_n = \frac{1}{2} = \frac{1}{2}\Delta\Sigma + \Delta G + L_q + L_G \quad (1)$$

where $\Delta\Sigma$ stands for the contribution from the quarks ($\Delta\Sigma = \Delta u + \Delta d + \Delta s$), ΔG is the contribution of the gluons and $L_{q,G}$ are their angular orbital momenta.

2 Experimental Procedure

COMPASS makes use of the SPS facilities, impinging a high intensity 160 GeV muon beam on a ⁶LiD polarised target. Besides the scattered muon, other particles produced

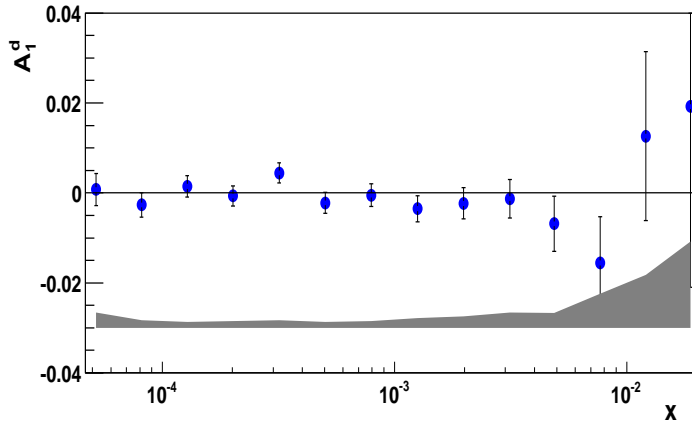


Figure 1: *The asymmetry $A_1^d(x)$ for quasi-real photons ($Q^2 < 1 \text{ (GeV/c)}^2$) as a function of x . The errors bars are the statistical ones. The grey band shows the systematic errors.*

in deep inelastic scattering are detected in a two-stage spectrometer. Data presented in this article have been collected in the years 2002, 2003 and 2004, corresponding to an integrated luminosity of about 2 fb^{-1} . The detailed description of the spectrometer can be found at Ref. [11].

3 The A_1^d Asymmetries

In order to access the spin-dependent structure function, g_1^d , the longitudinal photon-deuteron asymmetry, A_1^d , has to be evaluated. In the framework of the quark parton model this quantity can be directly related to the quark polarisation, Δq , via

$$A_1 = \frac{(\sigma_{\gamma\mu}^{\uparrow\downarrow} - \sigma_{\gamma\mu}^{\uparrow\uparrow})}{(\sigma_{\gamma\mu}^{\uparrow\downarrow} + \sigma_{\gamma\mu}^{\uparrow\uparrow})} \simeq \frac{\sum_q e_q^2 (\Delta q + \Delta \bar{q})}{\sum_q e_q^2 (q + \bar{q})} \quad (2)$$

where the arrows indicate the relative beam and target spin orientations. Figure 1 shows A_1^d as a function of x for quasi-real photon interactions for the data collected in the years 2002 and 2003. Events are selected by cuts on the four-momentum transfer squared ($Q^2 < 1 \text{ (GeV/c)}^2$) and the fractional energy of the virtual photon ($0.1 < y < 0.9$). Such a kinematic window allows a wide Bjorken scaling variable interval, $0.0005 < x < 0.02$ and provides more than 300 million events. The asymmetry is compatible with 0 over the whole x range. The error bars are the statistical ones and the grey band corresponds to systematic errors, which are due to false asymmetries mainly. Details on this analysis can be found in [12]. Figure 2 shows A_1^d as a function of x for DIS events ($Q^2 > 1 \text{ (GeV/c)}^2$), as measured by COMPASS using 2002, 2003 and 2004 data [13]. After data selection, 89×10^6 events are available for analysis. The results of the SMC [4], E143 [6], E155 [8] and HERMES [14] experiments are also shown. The asymmetry is 0 for $x < 0.05$ and gets larger as x increases, reaching 60% at $x \simeq 0.7$. The agreement is very good between the different data sets. It should be noted that only COMPASS and SMC

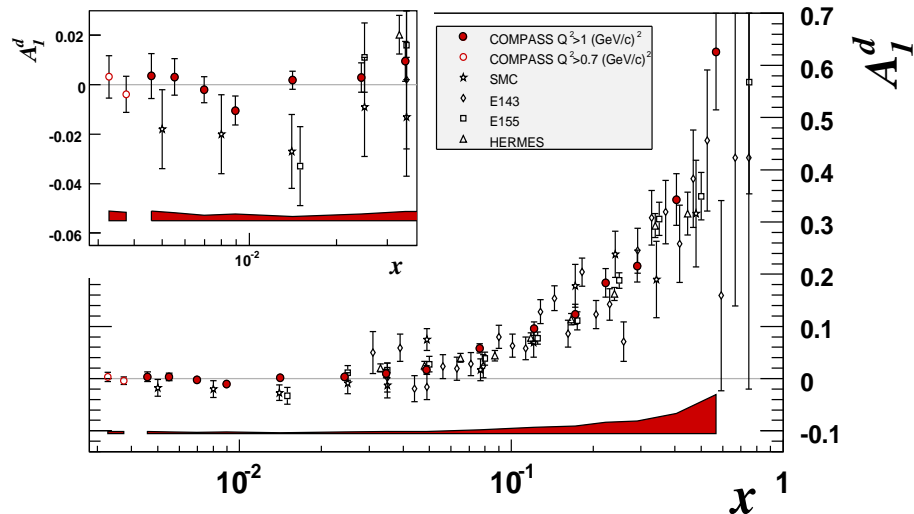


Figure 2: The asymmetry $A_1^d(x)$ as measured by the world spin experiments. The error bars are the statistical ones. The bands show the COMPASS systematic errors.

were able to measure this asymmetry at very low x , the COMPASS results being essential to disentangle the A_1^d behaviour at $x < 0.03$. Error bars are the statistical ones and the grey band corresponds to systematic errors of the COMPASS measurements, whose sources come from the uncertainty on beam and target polarisations (5% each), dilution factor (6%) and depolarisation factor (4-5%). Radiative corrections and the neglect of the transverse asymmetry A_2 are found to have a small effect. The upper limit for the systematic error due to false asymmetries is half of the statistical one.

4 The g_1^N Structure Function

The spin-dependent structure function of the nucleon, $g_1(x)$, is obtained from $A_1(x)$ and the spin-independent structure function $F_2(x)$ through

$$g_1(x) = A_1(x) \frac{F_2(x)}{2x(1+R)}, \quad (3)$$

where R is the ratio of the longitudinal to transverse photon absorption cross-sections. Figure 3 shows g_1^d as a function of x for DIS events [13]. The SMC results [4] have been evolved to the Q^2 of the corresponding COMPASS points. The two curves are the results of two QCD fits at the Q^2 of each data point. They are performed at NLO in the $\overline{\text{MS}}$ renormalisation and factorisation scheme. These fits require input parameterisations of the quark singlet spin distribution $\Delta\Sigma(x)$, non-singlet distributions $\Delta q_3(x)$ and $\Delta q_8(x)$, and the gluon spin distribution $\Delta G(x)$, which evolve according to the DGLAP equations. Data are well described by two solutions of DGLAP, with $\Delta G > 0$ and with $\Delta G < 0$. Figure 4 shows the QCD fit to proton, deuteron and neutron targets with positive ΔG solution (an indistinguishable curve is obtained for the solution with $\Delta G < 0$). All data

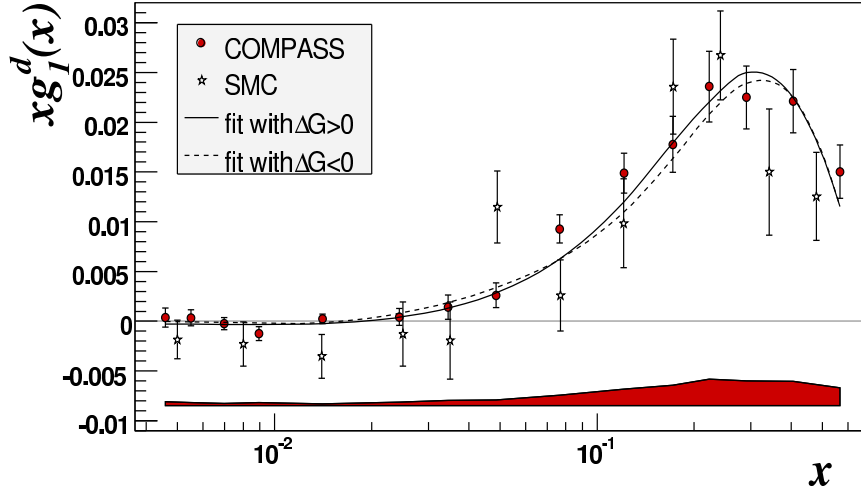


Figure 3: *The spin-dependent structure function of the deuteron, g_1^d , as a function of x ($Q^2 > 1$ (GeV/c) 2). The errors bars are the statistical ones. The band shows the COMPASS systematic errors. The curves show the results of QCD fits with $\Delta G > 0$ and $\Delta G < 0$.*

have been evolved to a common $Q_0^2 = 3$ (GeV/c) 2 , which corresponds to the average Q^2 of the COMPASS DIS data. The deuteron data are taken from Refs [4, 6, 8, 14], the proton data from Refs [4, 6, 14, 15, 16] and the ^3He data from Refs [10, 5, 17, 18]. For this analysis all bins, except the last one, have been subdivided into three Q^2 intervals. The number of COMPASS data points used in the fit to deuteron data is 43, out of a total of 230. Two different programs have been used to fit the data – one uses the DGLAP evolution equations for the spin structure functions in x and Q^2 phase space [20], the other uses the DGLAP evolution equations in the space of moments [21]. Both programs give consistent values of the fitted PDF parameters and similar χ^2 -probabilities. Although the shapes of the gluon distributions obtained with the two ΔG solutions differ over the whole x range, the fitted values of the first moment, η_G , are small and similar in absolute value $|\eta_G| \approx 0.2 - 0.3$. Similarly η_Σ reveals weak dependence on the shape of ΔG , being slightly larger in the fit with $\Delta G < 0$. The results from the two fits have been averaged

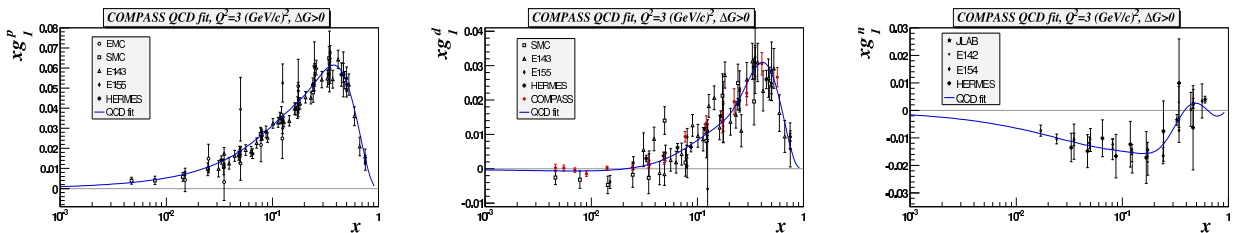


Figure 4: *The world data and QCD fit at $Q^2 = 3$ GeV^2 , obtained with the program of Ref. [20]. The curve corresponds to the solution with $\Delta G > 0$.*

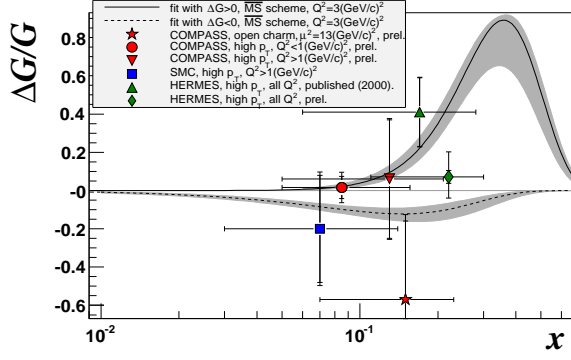


Figure 5: *Distribution of the gluon polarisation $\Delta G(x)/G(x)$ at $Q^2 = 3 \text{ (GeV/c)}^2$ for the fits with $\Delta G > 0$ and $\Delta G < 0$. Data points are taken from SMC [24], HERMES [22, 23] and COMPASS [25]. The error bars associated to the points are statistical. The error bands correspond to the statistical error on $\Delta G(x)$ at a given x .*

and give:

$$\eta_{\Sigma}(Q^2=3 \text{ (GeV/c)}^2) = 0.30 \pm 0.01(\text{stat.}) \pm 0.02(\text{evol.}). \quad (4)$$

In the \overline{MS} scheme η_{Σ} is identical to the matrix element a_0 , detailed below. The direct measurements of $\Delta G/G$, obtained at leading order in QCD, is compared with the indirect approach provided by the NLO QCD fits in figure 5. The unpolarised gluon distribution is taken from the MRST parameterisation [19]. The large statistical uncertainties of the direct measurements do not allow to disentangle between the two solutions for ΔG . More details on our QCD analysis can be found at Ref. [13].

We have calculated the integral of g_1^N using exclusively the experimental values of COMPASS evolved to $Q_0^2 = 3 \text{ GeV}^2$ and averaged over the two fits. Taking into account the contributions (2%, only) from the fits in the unmeasured regions of $x < 0.003$ and $x > 0.7$, we obtain:

$$\Gamma_1^N(Q^2=3 \text{ (GeV/c)}^2) = 0.050 \pm 0.003(\text{stat.}) \pm 0.003(\text{evol.}) \pm 0.005(\text{syst.}). \quad (5)$$

The second error accounts for the difference in Q^2 evolution between the two fits. The systematic error is the dominant one and mainly corresponds to the uncertainty on the beam and target polarisations and on the dilution factor. Γ_1^N is related to the matrix element of the singlet axial current a_0 , which measures the quark spin contribution to the nucleon spin. The relation between Γ_1^N and a_0 , now independent on Q^2 ($\hat{a}_0 = a_0(Q^2 \rightarrow \infty)$) (Ref. [26]), is

$$\Gamma_1^N(Q^2)_{Q^2 \rightarrow \infty} = \frac{1}{9} \hat{C}_1^S(Q^2) \hat{a}_0 + \frac{1}{36} C_1^{NS}(Q^2) a_8. \quad (6)$$

The coefficients \hat{C}_1^S and C_1^{NS} have been calculated in perturbative QCD up to the third order in $\alpha_s(Q^2)$ [26]. From the COMPASS result of Eq. 5 and taking the value of a_8 measured in hyperon β decay, assuming $SU(3)_f$ flavour symmetry ($a_8 = 0.585 \pm 0.025$ [27]), one obtains:

$$\hat{a}_0 = 0.33 \pm 0.03(\text{stat.}) \pm 0.05(\text{syst.}). \quad (7)$$

with the value of α_s evolved from the PDG value $\alpha_s(M_z^2) = 0.1187 \pm 0.005$. Combining this value with a_8 , the first moment of the strange quark distribution is:

$$(\Delta s(x) + \Delta \bar{s}(x))_{Q^2 \rightarrow \infty} = \frac{1}{3}(\hat{a}_0 - a_8) = -0.08 \pm 0.01(stat.) \pm 0.02(syst.). \quad (8)$$

One should keep in mind that the data have been evolved to a common Q^2 through a NLO fit, whereas the coefficients \hat{C}_1^S and C_1^{NS} , as well as $\alpha_s(Q^2)$, have been obtained beyond NLO. However, the choice of a value close to the average of Q^2 of the DIS data is expected to minimise the effect of the evolution in the results of \hat{a}_0 and $\Delta s(x) + \Delta \bar{s}(x)$ quoted above.

5 Valence Polarisations

In order to extract helicity distributions in LO QCD, unpolarised distributions and fragmentation functions for the hadron production from different quark flavours are needed:

$$A_1^h(x) = \frac{\sum_q e_q^2 (\Delta q(x) D_q^h + \Delta \bar{q}(x) D_{\bar{q}}^h)}{\sum_q e_q^2 (q(x) D_q^h + \bar{q}(x) D_{\bar{q}}^h)} \quad (9)$$

Figure 6 shows semi-inclusive asymmetries as a function of x for positive and negative unidentified charged hadrons. The kinematic range is basically the same as for inclusive analysis; in addition, the fraction of the photon energy carried out by the hadrons, z , is required to be between 0.2 and 0.85. COMPASS improves significantly the statistics with respect to SMC. A suitable way to get valence quark polarisations is to measure difference asymmetries [29, 30]. In LO QCD, under the assumption of isospin and charge conjugation symmetries, fragmentation functions do cancel out. Furthermore, for a deuteron target, no hadron identification is required, as difference asymmetries have the same expression both for pions and kaons:

$$A_N^{h^+ - h^-} = A_N^{\pi^+ - \pi^-} = A_N^{K^+ - K^-} = \frac{\Delta u_v + \Delta d_v}{u_v + d_v}, \quad (10)$$

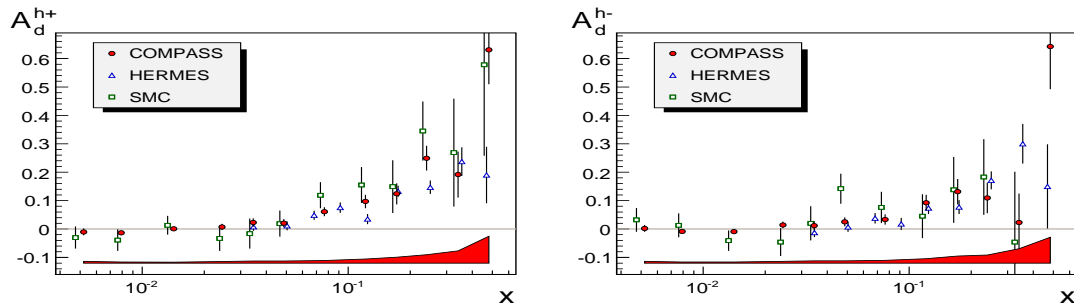


Figure 6: Hadron asymmetries $A_d^{h^+}$ (left) and $A_d^{h^-}$ (right) measured by COMPASS, SMC [28] and HERMES [14] experiments. The errors bars are the statistical ones. The band shows the COMPASS systematic errors.

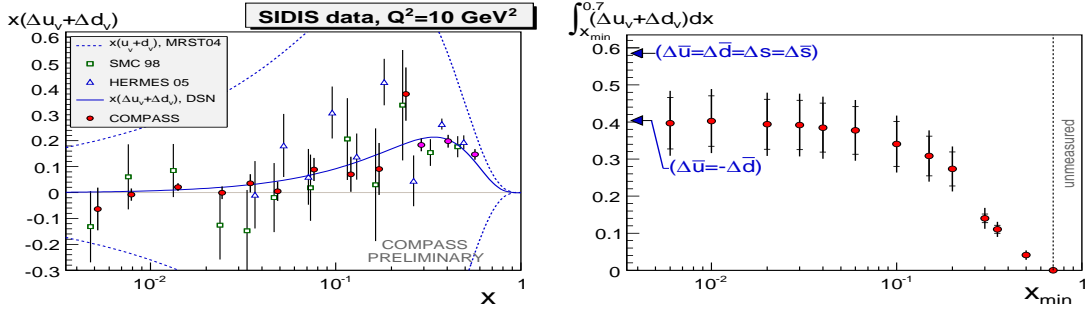


Figure 7: (Left) Polarised valence quark distribution $x(\Delta u_v(x) + \Delta d_v(x))$ for COMPASS, SMC [28] and HERMES [14]. The line shows the DNS fit which does not include the present COMPASS data. Three additional points at high x are obtained from g_1^d [13]. (Right) The integral of $\Delta u_v(x) + \Delta d_v(x)$ over the range $0.006 < x < 0.7$ as the function of x minimum, evaluated at $Q^2 = 10$ (GeV/c) 2 .

The measured single hadron asymmetries combined with the ratio of the charged hadron cross-sections are used to define difference asymmetries:

$$A^{h^+ - h^-} = \frac{1}{1 - r} (A^{h^+} - r A^{h^-}), \quad \text{with} \quad r = \frac{\sigma_{\uparrow\downarrow}^{h^-} + \sigma_{\uparrow\uparrow}^{h^-}}{\sigma_{\uparrow\downarrow}^{h^+} + \sigma_{\uparrow\uparrow}^{h^+}} = \frac{\sigma^{h^-}}{\sigma^{h^+}}. \quad (11)$$

The measured x range is slightly smaller as the r factor becomes 1 for $x < 0.006$. In order to determine the hadron acceptances a full chain Monte Carlo simulation is performed, in which the generated events face the same experimental conditions as real data do. Once the difference asymmetries are determined and knowing the unpolarised valence distributions the valence spin distributions are obtained from

$$\Delta u_v + \Delta d_v = \frac{(u_v + d_v)_{\text{MRST}}}{(1 + R)(1 - 1.5\omega_D)} A_d^{h^+ - h^-}. \quad (12)$$

For $x > 0.3$ the unpolarised sea contribution to F_2 vanishes and thanks to the positivity condition, $|\Delta q + \Delta \bar{q}| \leq |q + \bar{q}|$, the polarised sea contribution to the nucleon spin also becomes negligible in this region. These features allow the use of three points from the inclusive $g_1(x)$ COMPASS result [13] to define the valence polarisation. The advantage of this procedure is the gain in precision. A LO DNS analysis using KKP [31] fragmentations functions has been performed [32]. It includes all DIS g_1 results prior to COMPASS data, the partial COMPASS data on g_1 from Ref. [33] and all SIDIS results from SMC [28] and HERMES [14], where a symmetric sea in the valence range has been considered. Unpolarised MRST2004 [34] LO PDFs have been used. Figure 7(left) shows the comparison between COMPASS results and previous analyses from SMC and HERMES. All data points are evolved to a common $Q_0^2 = 10$ (GeV/c) 2 accordingly to DNS. The line stands for the DNS fit to SMC and HERMES data, only. Indeed, the COMPASS data agree very well with the other experiments and DNS parameterisation predicts successfully our result. Figure 7(right) shows the integral of the valence polarisation as a function of x minimum, evaluated at $Q_0^2 = 10$ (GeV/c) 2 . Its value over the measured x range (0.006 – 0.7) is $0.41 \pm 0.07(\text{stat.}) \pm 0.05(\text{sys.})$. The contribution from the upper unmeasured

region is estimated to be 0.004. Also the contribution from lower x values are expected to be small as the integral almost does not change for low x values.

The contribution of sea quarks to the nucleon spin can be obtained by combining the matrix elements a_0 and a_8 and the first moment of the valence polarisation:

$$\Delta\bar{u} + \Delta\bar{d} = (\Delta s + \Delta\bar{s}) + \frac{1}{2}(a_8 - \Gamma_v) = 3\Gamma_1^N - \frac{1}{2}\Gamma_v + \frac{1}{12}a_8 \quad (13)$$

The result shown in figure 7(right) favours an asymmetric scenario for the sea polarisation, $\Delta\bar{u} = -\Delta\bar{d}$, at a confidence level of two standard deviations, in contrast to the usual assumed symmetric scenario, $\Delta\bar{u} = \Delta\bar{d} = \Delta\bar{s} = \Delta s$. However, the statistical errors are still large and do not allow to draw firm conclusions. More details on this analysis can be found in [35].

6 Conclusions

COMPASS has measured the deuteron spin asymmetry A_1^d and its longitudinal spin-dependent structure function g_1^d with improved precision at $Q^2 < 1$ (GeV/c)² and $0.0005 < x < 0.02$, as well as $1 < Q^2 < 100$ (GeV/c)² and $0.004 < x < 0.7$. The measured DIS results have been evolved to a common Q^2 by a NLO QCD fit of the world g_1 data. The fit yields two solutions, one corresponding to $\Delta G(x) > 0$ and other to $\Delta G(x) < 0$, which describe the data equally well. The absolute values of the first moment of $\Delta G(x)$ are similar and not larger than 0.3. From the first moment Γ_1^N the matrix element of the singlet axial current \hat{a}_0 , in the limit $Q^2 \rightarrow \infty$, is found to be $0.33 \pm 0.03(stat.) \pm 0.05(syst.)$. The polarised valence quark distribution has been determined using the difference asymmetry approach in LO QCD. The integral at $Q_0^2=10$ (GeV/c)² over the measured x range, and including the extrapolation to the full x range, disfavors a symmetric sea at 2σ level and appoints to a opposite sign of $\Delta\bar{u}$ and $\Delta\bar{d}$.

References

- [1] M.J. Alguard *et al.* (E80 Coll.), Phys. Rev. Lett. **37**, 1261 (1976).
- [2] J.R. Ellis and R.L. Jaffe, Phys. Rev. D **9**, 1444 (1974).
- [3] J. Ashman *et al.* (EMC Coll.), Phys. Lett. B **206**, 364 (1988).
- [4] B. Adeva *et al.* (SMC Coll.), Phys. Rev. D **58**, 112001 (1998).
- [5] P.L. Anthony *et al.* (E142 Coll.), Phys. Rev. D **54**, 6620(1996).
- [6] K. Abe *et al.* (E143 Coll.) Phys. Rev. D **58**, 112003 (1998).
- [7] K. Abe *et al.* (E154 Coll.), Phys. Lett. B **405**, 180 (1997).
- [8] P.L. Anthony *et al.*, (E155 Coll.) Phys. Lett. B **463**, 339 (1999).
- [9] A. Airapetian *et al.* (HERMES Coll.), Phys. Lett. B **442**, 484 (1998).

- [10] X. Zheng *et al.* (JLAB/Hall A Coll.), Phys. Rev. Lett. **92** 012004 (2004).
- [11] P. Abbon *et al.*, (COMPASS Coll.), Nucl. Inst. Meth. A **577** (2007) 455.
- [12] V.Yu. Alexakhin *et al.* (COMPASS Coll.), Phys. Lett. B **647**, 330 (2007).
- [13] V.Yu. Alexakhin *et al.* (COMPASS Coll.), Phys. Lett. B **647**, 8 (2007).
- [14] A. Airapetian *et al.* (HERMES Coll.), Phys. Rev. D **75**, 012003 (2005)
- [15] P.L. Anthony *et al.* (E155 Coll.), Phys. Lett. B **493**, 19 (2000).
- [16] J. Ashman *et al.* (EMC Coll.), Nucl. Phys. B **328** (1989).
- [17] K. Abe *et al.* (E154 Coll.), Phys. Rev. Lett. **79**, 26 (1997).
- [18] K. Ackerstaff *et al.* (HERMES Coll.), Phys. Lett. B **404**, 383 (1997).
- [19] A. D. Martin, R. G. Roberts, W. J. Stirling and R. S. Thorne, Eur. Phys. J. C **4**, 463 (1998).
- [20] B. Adeva *et al.* (SMC Coll.), Phys. Rev. D **58** 112002 (1998).
- [21] A. N. Sissakian, O. Yu. Shevchenko and O. N. Ivanov, Phys. Rev. D **70**, 074032 (2004).
- [22] A. Airapetian *et al.*, (HERMES Coll.), Phys. Rev. Lett. **84**, 2584 (2000).
- [23] D. Hasch (HERMES Coll.), AIP Conf. Proc. **915**, 307 (2006).
- [24] B. Adeva *et al.*, (SMC Coll.), Phys. Rev. D **70**, 012002 (2004).
- [25] E. S. Ageev *et al.*, (COMPASS Coll.), Phys. Lett. B **633**, 25 (2006).
- [26] S. A. Larin *et al.*, Phys. Lett. B **404**, 153 (1997).
- [27] Y. Goto *et al.*, Phys. Rev. D **62**, 037503 (2003).
- [28] SMC Collaboration, B. Adeva *et al.*, Phys. Lett. B **420** (1998) 180.
- [29] L.L. Frankfurt *et al.*, Phys. Lett. B **230** (1989) 141.
- [30] E. Christova, E. Leader, Nucl. Phys. B **607** (2001) 369. Also these Proceedings.
- [31] B.A. Kniehl, G. Kramer, B. Potter, Nucl. Phys. B **582** (2000) 514.
- [32] D. de Florian, G.A. Navarro, R. Sassot, Phys. Rev. D **71** (2005) 094018.
- [33] E.S. Ageev *et al.*, (COMPASS Coll.) Phys. Lett. B **612** (2005) 154.
- [34] A.D. Martin, W.J. Stirling, R.S. Thorne, Phys. Lett. B **636** (2006) 259.
- [35] M. Alekseev *et al.* (COMPASS Coll.), CERN-PH-EP/2007-024, hep-ex/0707.4077, *subm. to Phys. Lett. B*.